J Arid Land (2025) 17(11): 1590–1603
doi: 10.1007/s40333-025-0059-x; CSTR: 32276.14.JAL.0250059x

Science Press Springer-Verlag

Determining groundwater-dependent ecological thresholds in the oasis–desert ecotone by exploring the linkage between plant communities and groundwater depth

CHANG Jingjing[1,2], ZENG Fanjiang[1,3,4], TAO Hui[1,2,4], WANG Shunke[1,3,4], LIU Xin[1,3,4], XUE Jie[1,3,4*]

[1] State Key Laboratory of Ecological Safety and Sustainable Development in Arid Lands, Xinjiang Institute of Ecology and Geography, Chinese Academy of Sciences, Urumqi 830011, China;
[2] Aksu National Station of Observation and Research for Oasis Agro-ecosystem, Aksu 843017, China;
[3] Cele National Station of Observation and Research for Desert–Grassland Ecosystems, Qira 848300, China;
[4] University of Chinese Academy of Sciences, Beijing 100049, China

Abstract: The diversity and discontinuity of plant communities in the oasis–desert ecotone are largely shaped by variations in groundwater depth, yet the relationships between spatial distribution patterns and ecological niches at a regional scale remain insufficiently understood. This study examined the oasis–desert ecotone in Qira County located in the Tarim Basin of China to investigate the spatial distribution of plant communities and groundwater depth as well as their relationships using an integrated approach that combined remote sensing techniques, field monitoring, and numerical modeling. The results showed that vegetation distribution exhibits marked spatial heterogeneity, with coverage ranked as follows: *Tamarix ramosissima*>*Phragmites australis*>*Populus euphratica*>*Alhagi sparsifolia*. Numerical simulations indicated that groundwater depths range from 2.00 to 65.00 m below the surface, with the system currently in equilibrium, sustaining an average annual recharge of 1.06×10^8 m^3 and an average annual discharge of 1.01×10^8 m^3. Groundwater depth strongly influences vegetation composition and structure: *Phragmites australis* dominates at average groundwater depth of 5.83 m, followed by *Populus euphratica* at average groundwater depth of 7.05 m. As groundwater depth increases, the community is initially predominated by *Tamarix ramosissima* (average groundwater depth of 8.35 m), then becomes a mixture of *Tamarix ramosissima*, *Populus euphratica*, and *Karelinia caspia* (average groundwater depth of 10.50 m), and finally transitions to *Alhagi sparsifolia* (average groundwater depth of 14.30 m). These findings highlight groundwater-dependent ecological thresholds that govern plant community composition and provide a scientific basis for biodiversity conservation, ecosystem stability, and vegetation restoration in the arid oasis–desert ecotone.

Keywords: oasis–desert ecotone; groundwater depth; vegetation community; *Tamarix ramosissima*; groundwater numerical model; Tarim Basin

Citation: CHANG Jingjing, ZENG Fanjiang, TAO Hui, WANG Shunke, LIU Xin, XUE Jie. 2025. Determining groundwater-dependent ecological thresholds in the oasis–desert ecotone by exploring the linkage between plant communities and groundwater depth. Journal of Arid Land, 17(11): 1590–1603. https://doi.org/10.1007/s40333-025-0059-x; https://cstr.cn/32276.14.JAL.0250059x

*Corresponding author: XUE Jie (E-mail: xuejie11@ms.xjb.ac.cn)
Received 2025-05-28; revised 2025-09-08; accepted 2025-09-15

1 Introduction

The oasis–desert ecotone is a critical component of the global dryland ecosystem (Ma et al., 2009; Mao et al., 2014; Xue et al., 2019; Ainiwaer et al., 2020; Chang et al., 2022). It is characterized as a transitional zone between oasis and desert, typically composed of a mosaic of ecosystems including grasslands, shrublands, and deserts. The vegetation types and distribution patterns in the oasis–desert ecotone are shaped by both natural and anthropogenic factors (Buerkert et al., 2005; Su et al., 2007; Buerkert et al., 2009; Pan et al., 2014; Mao et al., 2016; Zhang et al., 2019; Tariq et al., 2022). Among these factors, groundwater depth plays a decisive role in sustaining vegetation community distribution and ecological stability in the oasis–desert ecotone (Wei et al., 2008; Li et al., 2010; Rittner et al., 2016; Xue et al., 2019). Elucidating vegetation distribution and its association with groundwater depth is therefore essential for safeguarding this fragile ecosystem and ensuring long-term groundwater sustainability.

Vegetation composition in the oasis–desert ecotone is heterogeneous and discontinuous, with community distribution strongly influenced by fluctuations in groundwater depth (Bruelheide et al., 2003; Li et al., 2010; Soliman et al., 2019; Yin et al., 2023). Understanding the distribution features of desert plant communities and their responses to groundwater depth is critical for conserving biodiversity and achieving sustainable groundwater use in the oasis–desert ecotone (Zhao and Chang, 2014; Zhou et al., 2017; Xue et al., 2018; Brito et al., 2020; Han et al., 2023; Pan et al., 2024).

With the dual pressures of regional climate change and human activities, groundwater depth variation has become an increasing concern (Yin et al., 2023; Peng et al., 2024; Yang et al., 2024). Current research in the oasis–desert ecotone has largely concentrated on the effects of groundwater depth on the water physiological status of representative perennial species (Zhao and Wang, 2005; Yan et al., 2006; Zhang et al., 2020; Aili et al., 2023; Li et al., 2024; Gao et al., 2025). However, regional-scale studies examining the distribution characteristics of plant communities and their responses to groundwater variation remain limited.

This study investigated the distribution patterns of plant communities in the oasis–desert ecotone and their responses to groundwater depth. It further explored the associations between spatial distribution and ecological niches of desert plant communities. Specifically, using a combination of remote sensing techniques, field monitoring, and mathematical modeling, we analyzed spatial distribution and seasonal variation of vegetation types in relation to groundwater depth. The findings may provide scientific evidence for ecosystem management and policy design, offering guidance for biodiversity conservation, climate adaptation, and land-use planning. This study also has practical value for promoting stability and restoration of plant communities in peripheral oasis zones around the desert.

2 Study area and methods

2.1 Study area

The Qira oasis–desert ecotone (80°39′E–80°57′E, 36°55′N–37°08′N), located in the southern Tarim Basin of Xinjiang Uygur Autonomous Region, China, was selected as a representative study area due to its well-defined ecotone zoning and the availability of long-term monitoring data from the Cele National Station of Observation and Research for Desert–Grassland Ecosystems, Xinjiang Institute of Ecology and Geography, Chinese Academy of Sciences. Based on vegetation coverage in the Taklimakan Desert, Mu et al. (2013) defined areas with coverage between 20% and 25% as the oasis–desert ecotone. The oasis–desert ecotone lies downwind of the prevailing northwesterly and northeasterly winds of the Taklimakan Desert (Fig. 1) and is subject to frequent aeolian activity. The annual average number of dust days is 25.2 d, with a maximum of 59.0 d. The oasis–desert ecotone covers approximately 200.00 km^2 and is characterized by typical inland warm temperate desert climate with limited precipitation and frequent drought. The mean annual precipitation is 35.10 mm, whereas the mean annual potential

evaporation reaches 2600.00 mm. The dominant vegetation consists of xerophytic species such as *Tamarix ramosissima*, providing effective wind prevention and sand fixation functions and playing an important ecological protective role for farmland within the Qira oasis (Xue et al., 2016; Liu et al., 2018). The main soil types are aeolian sandy soil, brown desert soil, irrigated silty soil, and saline soil. Groundwater is a key determinant of vegetation distribution, with depth and fluctuations exerting strong effects on vegetation patterns, agriculture, ecosystem functions, and local socioeconomic conditions.

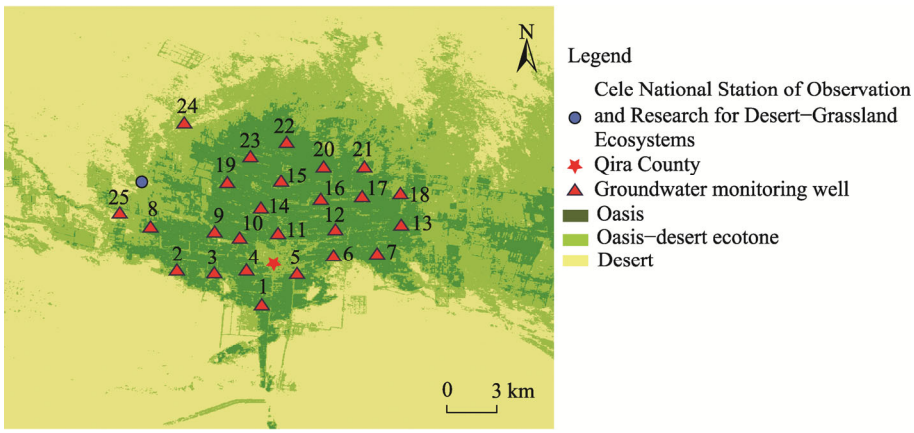

Fig. 1 Overview of the study area (Qira oasis–desert ecotone) and geographical locations of the groundwater monitoring wells

2.2 Data sources

Remote sensing data were obtained from Landsat 8-OLI (Geospatial Data Cloud Platform, Computer Network Information Center, Chinese Academy of Sciences; http://www.gscloud.cn) and Gaofen-1 products collected on August 24, 2023. Because satellite imagery is affected by weather conditions, only scenes with cloud cover <20% during the vegetation growing season were selected to ensure analytical accuracy. Image preprocessing, including spatial cropping, radiometric calibration, and atmospheric correction, was conducted using ENVI 5.3 (L3Harris Technologies, Inc., Melbourne, USA). High-resolution image interpretation in ENVI 5.3 followed a structured workflow of preprocessing, feature enhancement, classification, and post-processing. Further, images from July to September in 2023 were used to calculate the Normalized Difference Vegetation Index (NDVI) and vegetation coverage to capture peak vegetation growth (Zhang et al., 2019).

Based on the survey methods of Bruelheide et al. (2010) and Li et al. (2010), we chose three 100 m×100 m sampling plots to represent vegetation composition in the oasis–desert ecotone. The sampling plots were precisely located with a Global Positioning System (G28; UniStrong, Beijing, China). Within each sampling plot, all trees, shrubs, and grasses were inventoried using sampling measurement combined with GPS positioning and low-altitude unmanned aerial vehicle (UAV) photography. Recorded attributes included species composition, density (kg/m^3), height (m), coverage (m^2), aboveground biomass (kg/m^2), and belowground biomass (kg/m^2; 0–100 cm depth, including 0–20, 20–40, 40–60, 60–80, and 80–100 cm layers). Multispectral and Real-Time Kinematic (RTK) measurements were used to assess vegetation coverage and topographical variation. The UAV lens had a resolution exceeding 2000, producing imagery with a spatial resolution of <5 cm. UAV-based surveys provided a critical bridge between ground investigation and satellite data, supporting remote sensing inversion.

To capture plant species composition across the sampling plots, we conducted aerial photography using a DJI Phantom 4 RTK SE (CN) Combo (SZ DJI Technology Co., Ltd., Shenzhen, China) at an altitude of 500 m and with 20-megapixel resolution during 15–24 August

in 2023. Vertical images provided full coverage of the sampling plots and clearly displayed vegetation distribution and composition. Image processing and analysis of UAV data enabled extraction of plant species information, improving efficiency and yielding detailed ecological data without disturbing vegetation.

To analyze spatial distribution of plant communities and their association with groundwater depth, we collected groundwater data from 25 monitoring wells (Fig. 1) between 2008 and 2022. These long-term records, provided by the Cele National Station of Observation and Research for Desert–Grassland Ecosystems, supplied a continuous dataset for this study. Local hydrological parameters, such as water supply potential and irrigation seepage coefficients, were obtained from long-term field observations and experimental records. Further, hydrological (runoff) and meteorological (temperature, precipitation, and humidity) data spanning 2000–2019 were sourced from hydrological and meteorological stations located in the Qira oasis, providing by the Hotan Prefecture Water Resources Bureau.

2.3 Methods

2.3.1 Construction of groundwater numerical model

The Qira oasis covers an area of 145.00 km^2 and contains a porous subsurface water flow system with a homogeneous and unified hydraulic connection (Liu, 2019). The governing equation for the porous subsurface water flow system is as follows:

$$\begin{cases} \dfrac{\partial}{\partial x}\left[K(h-B)\dfrac{\partial h}{\partial x}\right]+\dfrac{\partial}{\partial y}\left[K(h-B)\dfrac{\partial h}{\partial y}\right]+\varepsilon_1(x,y,t)-\varepsilon_2(x,y,t)=\mu\dfrac{\partial h}{\partial t} & (x,y)\in D,\ t\geq 0 \\ h(x,y,0)=h_0(x,y) & (x,y)\in D \\ K(h-B)\dfrac{\partial h}{\partial n}|_{\Gamma_1}=q(x,y,t) & (x,y)\in \Gamma_1,\ t\geq 0 \end{cases}, \quad (1)$$

where x and y are the two-dimensional coordinates; t is the specific time (d); K is the permeability coefficient (m/d); h and B are the aquifer water level (m) and elevation (m), respectively; $\varepsilon_1(x, y, t)$ and $\varepsilon_2(x, y, t)$ are the recharge and discharge aquifer intensities at the three-dimensional scale (m/d), respectively; μ is the storage coefficient of the confined aquifer; D is the computational domain; $h(x, y, 0)$ is the water depth at the position (x, y) when the initial moment t is 0; $h_0(x, y)$ is the initial water level (m); n is the normal direction of the boundary; Γ_1 is the computational boundary condition; and $q(x, y, t)$ is the second-type boundary unit discharge (m^2/d).

2.3.2 Development and verification of groundwater numerical model

The development of groundwater numerical model comprises three main steps: model construction, parameter identification, and verification. In this study, Visual MODFLOW 4.6 (Waterloo Hydrogeologic, Waterloo, Canada) was used to establish the model. Visual MODFLOW 4.6 is a three-dimensional finite-difference simulation software designed for groundwater flow visualization. Its modular architecture enables researchers to select subroutine packages according to specific study requirements, offering both functionality and flexibility. The model employs an automatic rectangular grid division for spatial discretization, generating 11×10^3 grid cells, each with an area of 112 m×117 m. This grid resolution ensures sufficient accuracy and reliability of the simulation results.

Based on the analysis of aquifer burial conditions and hydraulic conductivity (Ma et al., 2019), we divided the study area into 18 parameter zones. This zoning accounts for geological heterogeneity, permeability, and storage capacity, thereby improving the representation of groundwater flow characteristics. The initial permeability values for each parameter zone were derived from comprehensive geological and hydrological datasets from the Water Resources Bulletin of Hotan Prefecture (Hotan Prefecture Water Resources Bureau, 2010–2020). Local hydrological parameters included water supply potential, irrigation seepage coefficients, and runoff, while meteorological data comprised temperature, precipitation, and humidity spanning

2000–2019. To further refine and validate the hydrological data, we employed groundwater monitoring instrument (PQWT-GT150A; Hunan Puqi Water Environment Research Institute Co., Ltd., Changsha, China) to collect the hydrogeological conditions and groundwater depth across the oasis–desert ecotone. These datasets enhanced the reliability and precision of the numerical groundwater simulation.

2.3.3 Calculation of groundwater recharge and discharge

According to the water balance of shallow groundwater, recharge sources include irrigation infiltration from oasis farmland, lateral infiltration from rivers, lateral groundwater inflow (or outflow), and recharge from canals and irrigation return flow (Liu, 2019). Groundwater discharge is mainly through evaporation, artificial exploitation, and subsurface lateral outflow.

Irrigation infiltration from oasis farmland is affected by lithology, groundwater level, and actual irrigation volume. The calculation formula is as follows:

$$Q_i = Q_s \times \beta , \tag{2}$$

where Q_i is the farmland irrigation seepage water (10^4 m^3/a); Q_s is the return flow from irrigation to groundwater (10^4 m^3/a); and β is the field infiltration coefficient reflecting the proportion of water that recharges the aquifer (Liu, 2019).

Lateral recharge from rivers can be estimated by quantifying water exchange between the river and aquifer:

$$Q_c = W \times l \times [K_c \times (B_c - g_r) / M] \times D_r , \tag{3}$$

where Q_c is the river-induced recharge (10^4 m^3/a), representing annual recharge from the river to groundwater; W is the riverbed width (m); l is the length of the river section (m); K_c is the permeability coefficient of bed deposits (m/d); B_c is the river water level (m); g_r is the groundwater level near the river (m); M is the thickness of the riverbed deposits (m); and D_r is the duration of recharge (d).

According to Darcy's law, we calculated lateral groundwater inflow (or outflow) as Equation 4 (Liu, 2019):

$$Q_g = \rho \times \gamma \times \varphi \times \omega \times \Delta T , \tag{4}$$

where Q_g is the lateral groundwater inflow or outflow (10^4 m^3/a); ρ is the aquifer permeability coefficient (m/d); γ is the hydraulic gradient; φ is the cross-sectional width (m); ω is the aquifer thickness (m); and ΔT is the calculation time (d).

Recharge from canals and irrigation return flow can be estimated as:

$$Q_q = (1 - N') \times Q_y \times r , \tag{5}$$

where Q_q is the canal system infiltration recharge (10^4 m^3/a); N' is the effective utilization coefficient of the canal system; Q_y is the amount of water diverted from the canal head (10^4 m^3/a); and r is a correction factor to account for local drainage behavior (typically 0.90).

Groundwater evaporation can be calculated using Avilyanov's formula (Liu, 2019):

$$Q_z = F \times \varepsilon_0 \times (1 - \Delta / \Delta_0)^{l_d} , \tag{6}$$

where Q_z is the groundwater evaporation loss (10^4 m^3/a); F is the area with shallow groundwater depth (10^4 m^2); ε_0 refers to the surface water evaporation intensity; Δ is the evaporation adjustment factor; Δ_0 is the groundwater evaporation limit depth (m), above which evaporation can be ignored; and l_d is a lithology-dependent index. Different lithologies have different control effects on water movement and evaporation.

In the oasis irrigation district, 25 irrigation wells extract approximately 0.60×10^8 m^3 of water annually. Of this volume, 88% is used for agriculture, with the remainder allocated to industrial, domestic, and urban greening purposes (Hotan Prefecture Water Resources Bureau, 2010–2020). The effective utilization coefficient of electromechanical wells is set to 0.85 in this study, indicating that 85% of pumped water is effectively consumed. The field irrigation infiltration

coefficient is set to 0.08, meaning that 8% of irrigation water recharges groundwater. These coefficients can quantify water use efficiency and the proportion of recharge under current management practices (Liu, 2019).

2.3.4 Data analysis

In this study, spatiotemporal changes in plant communities within the oasis–desert ecotone were assessed through a combination of remote sensing interpretation and field survey sampling. Groundwater dynamics were simulated using the Visual MODFLOW 4.6 numerical model. ArcGIS v.16.0 software was employed to generate spatial distribution maps, and SigmaPlot v.14.0 software was used to produce statistical charts of the analyzed variables.

3 Results

3.1 Distribution characteristics of plant communities in the oasis–desert ecotone

Figure 2 illustrates the spatial distribution of plant communities in the oasis–desert ecotone. The dominant perennial communities included *Tamarix ramosissima*, *Phragmites australis* (syn. *Phragmites communis*), *Populus euphratica*, and *Alhagi sparsifolia*. These communities covered large areas and played a vital role in sand stabilization at the oasis margin. The *Karelinia caspia* community was mainly distributed along dune edges and undulating sandy areas at the oasis periphery. Community dominated by *Alhagi sparsifolia* occurred in the western and northern parts of the oasis, particularly along flat sandy terrain, low dunes, and high dunes. *Phragmites australis* community was concentrated in areas with high groundwater tables or where groundwater is readily replenished.

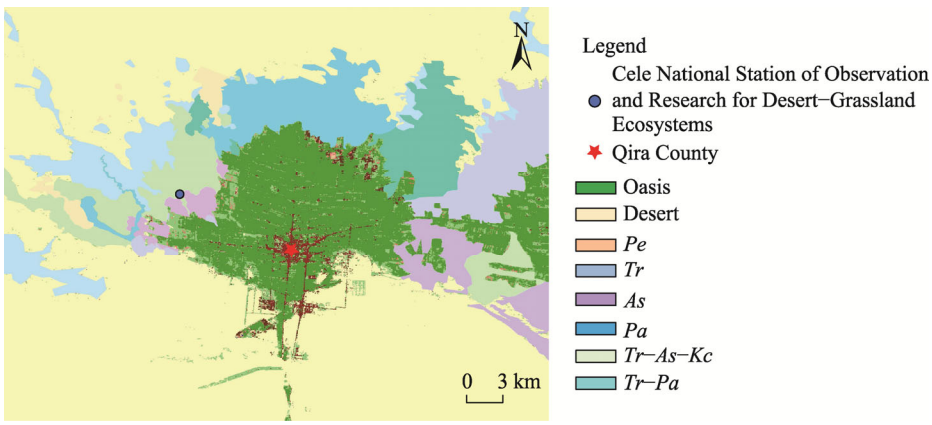

Fig. 2 Distribution of main vegetation communities in the Qira oasis–desert ecotone based on GF-1 satellite images. *Pe*, *Populus euphratica*; *Tr*, *Tamarix ramosissima*; *As*, *Alhagi sparsifolia*; *Pa*, *Phragmites australis*; *Tr–As–Kc*, *Tamarix ramosissima–Alhagi sparsifolia–Karelinia caspia*; *Tr–Pa*, *Tamarix ramosissima–Phragmites australis*.

Multiple surveys and validation based on Bruelheide et al. (2010) and Li et al. (2010) confirmed these patterns. As shown in Figure 2, vegetation distribution and the area of each community type varied considerably across the study area. Dominant communities were concentrated in central farmland and construction zones. Among single community types, *Tamarix ramosissima–Phragmites australis* covered the largest area (82.59 km^2). Its distribution was concentrated in the northwest, extending southeastward. *Phragmites australis* community covered 74.04 km^2, primarily in the central–northern region. *Tamarix ramosissima–Alhagi sparsifolia–Populus euphratica* occupied 75.31 km^2, mainly in the northeastern and southeastern parts, as well as in the western and central–northern areas. Among all species studied, *Populus euphratica* and *Alhagi sparsifolia* had the smallest distributions, covering 13.32 and 12.30 km^2,

respectively. *Populus euphratica* occurred as single stands in the western part and in mixed community (*Tamarix ramosissima–Alhagi sparsifolia–Populus euphratica*) in the western and northern regions. Collectively, these plant communities formed a natural buffer between oasis and desert, playing an essential role in maintaining oasis stability.

3.2 Change and simulation of groundwater depth in the oasis–desert ecotone

Since joining the national field station observation network in 2005, the Cele National Station of Observation and Research for Desert–Grassland Ecosystems has maintained two long-term groundwater monitoring wells in farmland and desert areas near the research station to record monthly groundwater fluctuations. Results indicated that oasis groundwater displays both seasonal variability and notable interannual changes. In traditional oasis zones, groundwater generally remains in dynamic equilibrium. However, in northwestern areas undergoing expansion and reclamation, a local decline in groundwater depth has been observed, with decreases of 0.09 m/a (Fig. 3).

In 2008, 25 additional groundwater monitoring wells were installed across the oasis region to record groundwater depths bimonthly to improve understanding of groundwater dynamics. Average groundwater depth across the oasis region ranged from 2.00 to 65.00 m, decreasing gradually from the south and west toward the east due to geological conditions. Analysis of interannual groundwater depth from these monitoring wells showed that resources at the oasis scale are currently secure. However, unstable trends in the northwestern part could, if aggravated, pose risks to the overall water security (Fig. 4).

Numerical model calibration through parameter adjustment, flow field fitting, and hydrogeological validation yielded satisfactory results (Fig. 5). The maximum absolute fitting error of flow field was 1.36 m and the mean absolute error was 0.35 m, indicating strong agreement between simulated and observed flow fields. Minor deviations were attributed to uncertainties in estimating extraction volumes but were within acceptable limits.

Simulation results showed an average annual recharge of 1.06×10^8 m^3 and an average annual discharge of 1.01×10^8 m^3, with groundwater extraction accounting for 60% (Fig. 6). These findings suggested that the current groundwater use in the oasis region is relatively safe. According to the Water Resources Bulletin of Hotan Prefecture (Hotan Prefecture Water Resources Bureau, 2010–2020), sustainable groundwater extraction corresponds to approximately 70% of recharge, or about 0.64×10^8 m^3 annually. Current groundwater extraction in the irrigation area is about 0.60×10^8 m^3 annually, falling within the safe threshold. However, the results also emphasized the need for prudent water management to prevent overexploitation.

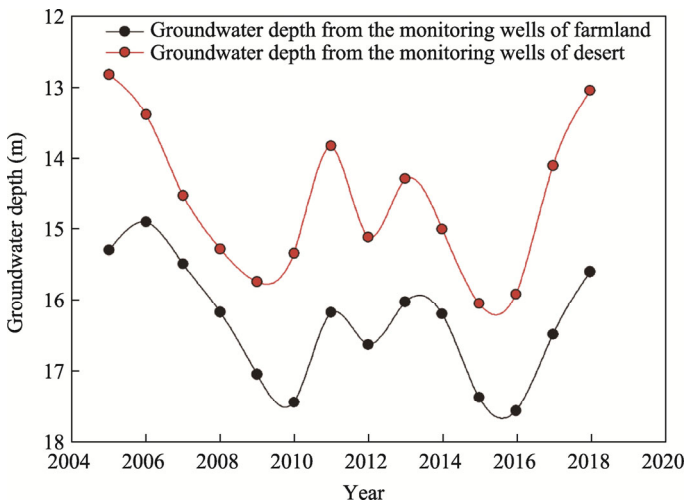

Fig. 3 Variation in observed groundwater depth across the Qira oasis and desert in recent years

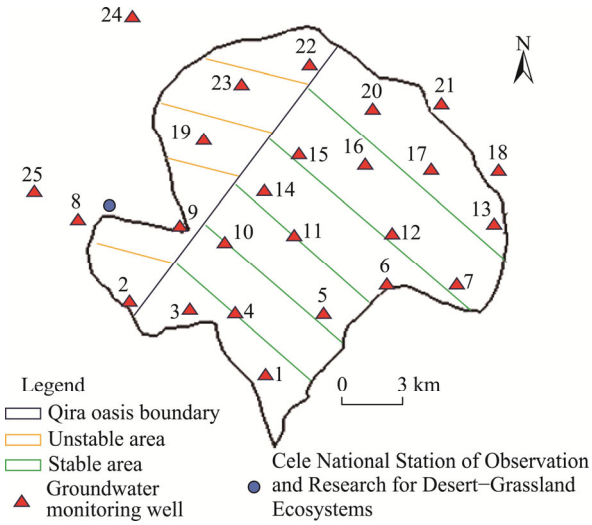

Fig. 4 Zones with stable and unstable groundwater depth in the Qira oasis

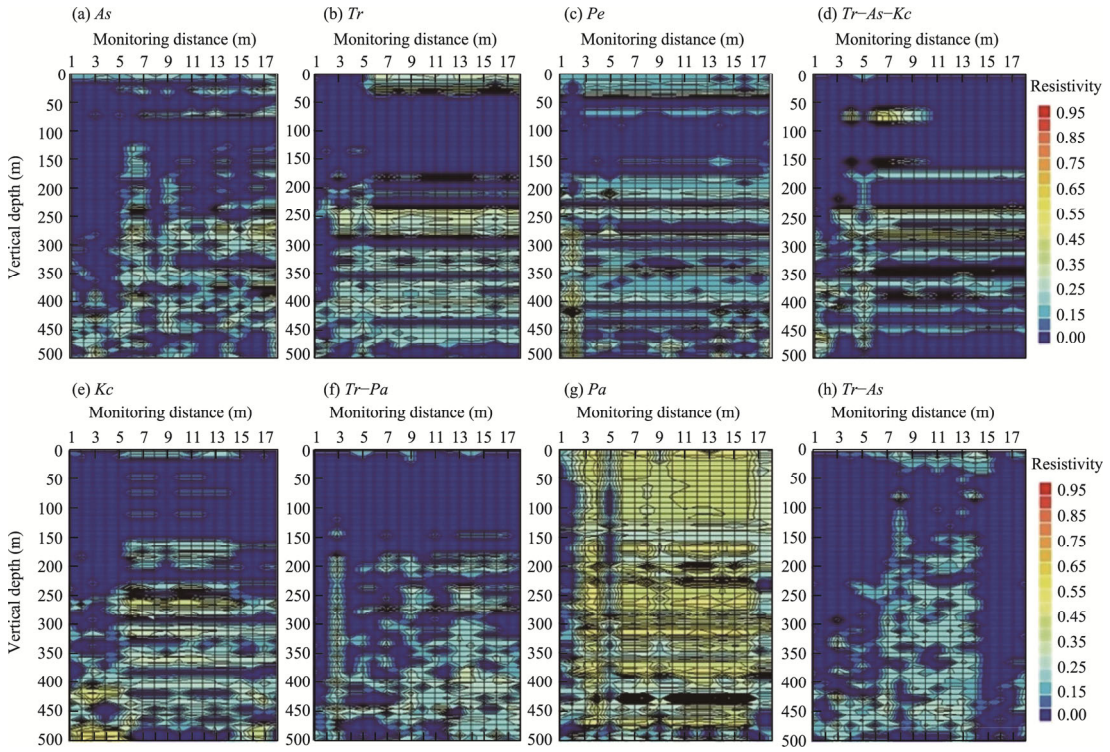

Fig. 5 Hydrogeological groundwater monitoring in different plant community areas of the oasis–desert ecotone. (a), *As* (*Alhagi sparsifolia*); (b), *Tr* (*Tamarix ramosissima*); (c), *Pe* (*Populus euphratica*); (d), *Tr–As–Kc* (*Tamarix ramosissima–Alhagi sparsifolia–Karelinia caspia*); (e), *Kc* (*Karelinia caspia*); (f), *Tr–Pa* (*Tamarix ramosissima–Phragmites australis*); (g), *Pa* (*Phragmites australis*); (h), *Tr–As* (*Tamarix ramosissima–Alhagi sparsifolia*).

Under the present oasis scale and prevailing flood irrigation practices, annual extraction of 0.60×10^8 m^3 groundwater can sustain both surface water and groundwater security. Nevertheless, groundwater depths in the expansion areas of the oasis, particularly along the southwestern margin of the oasis–desert ecotone, showed a downward trend. This indicated that large-scale expansion of the oasis is not advisable under current inflow conditions and safe extraction limits.

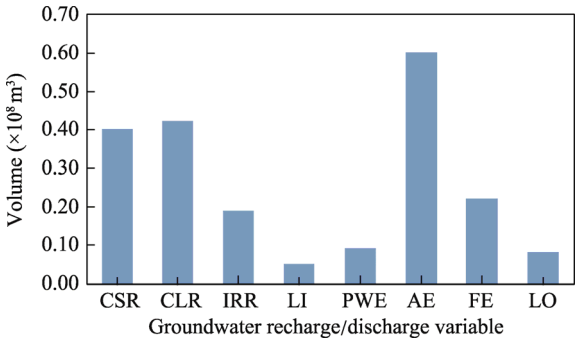

Fig. 6 Groundwater recharge and discharge in the oasis irrigation area. CSR, CLR, IRR, and LI refer to variables of groundwater recharge including channel seepage recharge, canal leakage recharge, irrigation reinfiltration recharge, and lateral inflow, respectively. PWE, AE, FE, and LO stand for phreatic water evaporation, artificial exploitation, farm evapotranspiration, and lateral outflow, respectively.

3.3 Response of vegetation community distribution in the oasis–desert ecotone to groundwater depth

In the oasis–desert ecotone, natural vegetation is strongly associated with groundwater depth. This reflects the arid climate of the region, where precipitation is minimal and groundwater serves as the primary water source for plant growth. In the oasis region, most river water is diverted for farmland irrigation, which greatly limits surface water replenishment for natural vegetation. Therefore, groundwater is the critical resource supporting vegetation survival and ecological stability.

Field survey and sampling data from plant communities under different groundwater depths (Fig. 7) showed that *Phragmites australis* dominated areas with shallow groundwater between 2.80–8.86 m (average groundwater depth of 5.83 m), demonstrating its ability to sustain growth using near-surface groundwater. With increasing groundwater depth, plant community composition became more diverse, with *Tamarix ramosissima*, *Populus euphratica*, and *Phragmites australis* coexisting, indicating differentiation in water requirements and interspecific adaptability.

When groundwater depth ranged between 4.00 and 10.10 m (average of 7.05 m), *Populus euphratica* was the dominant species, highlighting its strong tolerance to deeper groundwater. At groundwater depths of 2.90–13.80 m (average of 8.35 m), *Tamarix ramosissima* was prevalent, reflecting its adaptability and competitive advantage in medium to deep groundwater

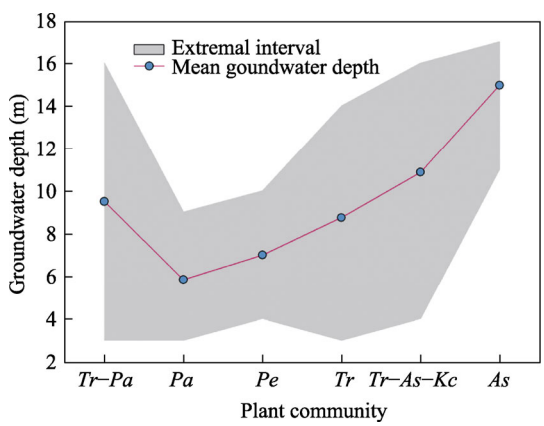

Fig. 7 Relationship between groundwater depth and main plant communities in the oasis–desert ecotone. *Tr–Pa*, *Tamarix ramosissima–Phragmites australis*; *Pa*, *Phragmites australis*; *Pe*, *Populus euphratica*; *Tr*, *Tamarix ramosissima*; *Tr–As–Kc*, *Tamarix ramosissima–Alhagi sparsifolia–Karelinia caspia*; *As*, *Alhagi sparsifolia*.

environments. At groundwater depths of 4.20–16.80 m (average of 10.50 m), the community was composed of *Tamarix ramosissima–Alhagi sparsifolia–Karelinia caspia*. When groundwater depth was between 11.20 and 17.40 m (average of 14.30 m), *Alhagi sparsifolia* replaced other plant species as the dominant species, demonstrating its drought resistance and capacity to survive under extremely deep groundwater conditions. The order of groundwater depth across dominant communities was greatest under *Alhagi sparsifolia*, followed by *Tamarix ramosissima*, *Populus euphratica*, and *Phragmites australis*. Therefore, substantial groundwater decline would severely threaten species such as *Phragmites australis*, which depend heavily on shallow groundwater (Fig. 7).

4 Discussion

In the oasis–desert ecotone outside the oasis region of Qira County, plant communities exhibit an orderly spatial distribution in response to groundwater depth. This pattern reflects the capacity of plant communities to adjust their composition and structure according to groundwater availability, enabling adaptation to varying depths. Groundwater depth, as a key ecological factor, directly influences plant growth and distribution and thus determines vegetation type and density (Bruelheide et al., 2010; Li et al., 2010; Chang et al., 2022).

Changes in groundwater depth regulate the spatial regularity of vegetation distribution, resulting in a multilayered and diverse ecological landscape (Faure et al., 2002; Bruelheide et al., 2010). *Alhagi sparsifolia* community dominates in areas with the deepest groundwater, reflecting its adaptability to relatively deep groundwater environments. As groundwater depths rise, *Tamarix ramosissima* persists and combines with other plant species, forming dynamic community patterns. With shallower groundwater, *Phragmites australis* and *Tamarix ramosissima* communities become prominent, while *Phragmites australis* community dominates in areas with the shallowest groundwater, indicating species-specific groundwater preferences. Across these groundwater depth gradients, vegetation forms distinct assemblages, including perennial herbaceous, shrub, tree, shrub–herbaceous, and herbaceous communities. While broadly similar to vegetation types in temperate desert mountains, these assemblages are more complex and unique due to the extreme aridity (Luo et al., 2003; Zhao et al., 2019; Chang et al., 2022).

Comparable patterns have been reported in other oasis–desert regions of China such as the Ejin oasis and the Tarim River basin, where groundwater depth drives vegetation succession from herbaceous communities reliant on high water levels to tree- and shrub-dominated communities (Ma et al., 2003; Xie et al., 2014; Song and Zhang, 2015; Zhou et al., 2016; Zhang et al., 2017). However, in extremely arid areas such as Qira County, plant communities are characterized by simpler structures and fewer species, constrained by harsh environmental conditions (Bruelheide et al., 2003; Li et al., 2010). In areas with very deep groundwater, vegetation mainly persists in phreatophytic communities, which differ markedly in traits and adaptations from common xerophytes such as *Haloxylon ammodendron* and *Tamarix ramosissima*. This highlights both the strong dependence of desert vegetation on groundwater and the distinctive distribution patterns shaped under extreme aridity conditions (Bruelheide et al., 2003; Luedeling and Buerkert, 2008; Chang et al., 2022).

Notably, as groundwater depths continue to decline, vegetation does not transition into shrub or dwarf-shrub communities but often shifts to perennial herbaceous assemblages (Li et al., 2010). This reflects how groundwater reduction in extremely arid environments alters plant community structure, with cascading effects on ecosystem stability and biodiversity (Bruelheide et al., 2010; Meng et al., 2016). These findings provide a scientific basis for understanding vegetation succession in arid regions and have practical implications for ecological protection and water resource management in desert environments.

This study highlights the distribution characteristics of plant communities in the oasis–desert ecotone and their dependence on groundwater depth, with important implications for conservation and sustainable management. However, vegetation distribution is also shaped by soil moisture,

landform, climate, etc. (Xie et al., 2014; Tydecks et al., 2023). Soil water directly affects plant survival, topography governs water accumulation and loss, and climate provides the fundamental conditions for plant growth (Li et al., 2010; Guezoul et al., 2013; Moat et al., 2021; Chang et al., 2022). These factors interact to form a complex ecosystem that regulates plant community structure and function.

5 Conclusions

Using UAV monitoring, ground sampling, groundwater monitoring, and numerical modeling, this study analyzed the relationship between vegetation community distribution and groundwater depth during 2023–2024 in the Qira oasis–desert ecotone in the southern margin of the Tarim Basin. Results showed that plant communities in the oasis–desert ecotone exhibited marked spatial heterogeneity. Communities were centered around farmland and construction zones. Analysis of the distribution areas of individual vegetation community types showed that coverage, from largest to smallest, was as follows: *Tamarix ramosissima>Phragmites australis>Populus euphratica>Alhagi sparsifolia*. Groundwater depth in the oasis region ranged from 2.00 to 65.00 m. Numerical simulations indicated that the groundwater system is currently in a balanced state, with an average annual recharge of 1.06×10^8 m^3 and an average annual discharge of 1.01×10^8 m^3 during the simulation period. Plant community composition and structure varied according to groundwater depth. Specifically, *Phragmites australis* dominated in areas with average groundwater depth of 5.83 m. At groundwater depths of 4.20–16.80 m, the community was composed of *Tamarix ramosissima–Alhagi sparsifolia–Karelinia caspia*, while *Populus euphratica* was dominant when groundwater depths were between 4.00 and 10.10 m. At average groundwater depth of 8.35 m, *Tamarix ramosissima* became the prevailing plant species, whereas at average groundwater depth of 14.30 m, *Alhagi sparsifolia* had an absolute advantage. Future research should integrate soil–plant–groundwater interactions across multiple factors, spatial scales, and temporal processes to establish robust models for quantifying the associations between desert vegetation and groundwater in the oasis–desert ecotone.

Conflict of interest

The authors declare that they have no known competing financial interests or personal relationships that could have appeared to influence the work reported in this paper.

Acknowledgements

This work was financially supported by the Tianchi Talents Program of Xinjiang Uygur Autonomous Region (E5358525; 2025–2026), the Major Science and Technology Special Project of Xinjiang Uygur Autonomous Region (2024A03009-4), the Third Xinjiang Scientific Expedition Program (2022xjkk010402), the National Key Research and Development Program of China (2022FY202305-06), the Tianshan Talents Program of Xinjiang Uygur Autonomous Region (2022TSYCJU0002), and the Outstanding Member of the Youth Innovation Promotion Association of the Chinese Academy of Sciences (2019; 2024–2026).

Author contributions

Conceptualization: CHANG Jingjing, ZENG Fanjiang, TAO Hui, XUE Jie; Methodology: CHANG Jingjing, ZENG Fanjiang, TAO Hui, XUE Jie; Software: CHANG Jingjing; Validation: CHANG Jingjing; Formal analysis: CHANG Jingjing; Supervision: ZENG Fanjiang, TAO Hui, XUE Jie; Writing - original draft preparation: CHANG Jingjing; Writing - review and editing: ZENG Fanjiang, TAO Hui, XUE Jie; Data Curation and Visualization: WANG Shunke, LIU Xin. All authors approved the manuscript.

References

Aili A, Xu H L, Xu Q, et al. 2023. Aeolian dust movement and deposition under local atmospheric circulation in a desert-oasis transition zone of the northeastern Taklimakan desert. Ecological Indicators, 157: 111289, doi:

10.1016/j.ecolind.2023.111289.

Ainiwaer M, Ding J L, Kasim N. 2020. Deep learning-based rapid recognition of oasis-desert ecotone plant communities using UAV low-altitude remote-sensing data. Environmental Earth Sciences, 79(10): 216, doi: 10.1007/s12665-020-08965-w.

Brito J C, Pleguezuelos J M. 2020. Desert biodiversity—world's hot spots/globally outstanding biodiverse deserts. Encyclopedia of the World's Biomes, 2–5: 10–22.

Bruelheide H, Jandt U, Gries D, et al. 2003. Vegetation changes in a river oasis on the southern rim of the Taklamakan Desert in China between 1956 and 2000. Phytocoenologia, 33(4): 801–818.

Bruelheide H, Vonlanthen B, Jandt U, et al. 2010. Life on the edge-to which degree does phreatic water sustain vegetation in the periphery of the Taklamakan Desert? Applied Vegetation Science, 13(1): 56–71.

Buerkert A, Nagieb M, Siebert S, et al. 2005. Nutrient cycling and field-based partial nutrient balances in two mountain oases of Oman. Field Crops Research, 94(2–3): 149–164.

Buerkert A, De Langhe E, Al Khanjari S. 2009. Ecology and morphological traits of an ancient *Musa acuminata* cultivar from a mountain oasis of Oman. Genetic Resources and Crop Evolution, 56(5): 609–614.

Chang J J, Gong L, Zeng F J, et al. 2022. Using hydro-climate elasticity estimator and geographical detector method to quantify the individual and interactive impacts on NDVI in oasis-desert ecotone. Stochastic Environmental Research and Risk Assessment, 36: 3131–3148.

Faure H, Walter R C, Grant D R. 2002. The coastal oasis: Ice age springs on emerged continental shelves. Global and Planetary Change, 33(1–2): 47–56.

Gao F, Lv K X, Jiang Q O, et al. 2025. How did the regional water-heat distribution in oasis area vary with the different spatial patterns and structures of shelterbelt system—A case study in Ulan Buh desert oasis. Agricultural and Forest Meteorology, 362: 110345, doi: 10.1016/j.agrformet.2024.110345.

Guezoul O, Chenchouni H, Sekour M, et al. 2013. An avifaunal survey of mesic manmade ecosystems "Oases" in Algerian hot-hyperarid lands. Saudi Journal of Biological Sciences, 20(1): 37–43.

Han W Q, Guan J Y, Zheng J H, et al. 2023. Probabilistic assessment of drought stress vulnerability in grasslands of Xinjiang, China. Frontiers in Plant Science, 14: 1143863, doi: 10.3389/fpls.2023.1143863.

Hotan Prefecture Water Resources Bureau. 2010–2020. Water Resources Bulletin of Hotan Prefecture. Hotan: Hotan Prefecture Water Resources Bureau. (in Chinese)

Li W, Shen Y, Wang G H, et al. 2024. Plant species diversity and functional diversity relations in the degradation process of desert steppe in an arid area of northwest China. Journal of Environmental Management, 365: 121534, doi: 10.1016/j.jenvman.2024.121534.

Li X Y, Lin L S, Zhang X M, et al. 2010. Influence of groundwater depth on species composition and community structure in the transition zone of Cele oasis. Journal of Arid Land, 2(4): 235–242.

Liu Y, Xue J, Gui D W, et al. 2018. Agricultural oasis expansion and its impact on oasis landscape patterns in the southern margin of Tarim basin, Northwest China. Sustainability, 10(6): 1957, doi: 10.3390/su10061957.

Liu Y. 2019. Combined utilization research of surface water and groundwater in oasis irrigation district of southern margin of Tarim Basin—a case study of Cele oasis. PhD Dissertation. Urumqi: Xinjiang University. (in Chinese)

Luedeling E, Buerkert A. 2008. Typology of oases in northern Oman based on Landsat and SRTM imagery and geological survey data. Remote Sensing of Environment, 112(3): 1181–1195.

Luo G P, Chen X, Zhou K F, et al. 2003. Temporal and spatial variation and stability of the oasis in the Sangong River Watershed, Xinjiang, China. Science in China Series D-Earth Sciences, 46(1): 62–73.

Ma M G, Wang X M, Cheng G D. 2003. Study on the oasis corridor landscape in the arid regions based on RS and GIS methods—application of Jinta Oasis, China. Journal of Environmental Sciences, 15(2): 193–198.

Ma Q L, Wang J H, Li X R, et al. 2009. Long-term changes of *Tamarix*-vegetation in the oasis-desert ecotone and its driving factors: Implication for dryland management. Environmental Earth Sciences, 59: 765–774.

Ma T, Wang J W, Liu Y, et al. 2019. A mixed integer linear programming method for optimizing layout of irrigated pumping well in oasis. Water, 11(6): 1185, doi: 10.3390/w11061185.

Mao D L, Lei J Q, Zeng F J, et al. 2014. Characteristics of wind erosion and deposition in oasis-desert ecotone in southern margin of Tarim Basin, China. Chinese Geographical Science, 24: 658–673.

Mao D L, Lei J Q, Zhao Y, et al. 2016. Effects of variability in landscape types on the microclimate across a desert-oasis region on the southern margins of the Tarim Basin, China. Arid Land Research and Management, 30(1): 89–104.

Meng B, Gui D W, Zeng F J, et al. 2016. Spatio-temporal variability of oasis groundwater in southern rim of Tarim basin and

monitoring sites optimization—a case study in Cele oasis. Bulletin of Soil and Water Conservation, 36(2): 209–215. (in Chinese)

Moat J, Orellana-Garcia A, Tovar C, et al. 2021. Seeing through the clouds-Mapping desert fog oasis ecosystems using 20 years of MODIS imagery over Peru and Chile. International Journal of Applied Earth Observation and Geoinformation, 103(1–4): 102468, doi: 10.1016/j.jag.2021.102468.

Mu G J, He J X, Lei J Q, et al. 2013. A discussion on the transitional zone from oasis to sandy desert: A case study at Cele oasis. Arid Land Geography, 36(2): 195–202. (in Chinese)

Pan G Y, Gui J, Yue J, et al. 2014. Change of the oasis-desert ecotone and its causes in Qira County during the period of 2001–2010. Arid Zone Research, 31(1): 169–175. (in Chinese)

Pan J P, Zhang K C, An Z S, et al. 2024. Near-surface wind field characteristics of the desert-oasis transition zone in Dunhuang, China. Journal of Arid Land, 16(5): 654–667.

Peng L, Wan Y B, Li H, et al. 2024. Influence of surface water and groundwater gradient on spatial distribution of typical vegetation in the hinterland of Taklamakan desert. Science of the Total Environment, 953: 176060, doi: 10.1016/j.scitotenv.2024.176060.

Rittner M, Vermeesch P, Carter A, et al. 2016. The provenance of Taklamakan desert sand. Earth and Planetary Science Letters, 437: 127–137.

Soliman S S M, Abouleish M, Abou-Hashem M M M, et al. 2019. Lipophilic metabolites and anatomical acclimatization of *Cleome amblyocarpa* in the drought and extra-water areas of the arid desert of UAE. Plants, 8(5): 132, doi: 10.3390/plants8050132.

Song W, Zhang Y. 2015. Expansion of agricultural oasis in the Heihe River Basin of China: Patterns, reasons and policy implications. Physics and Chemistry of the Earth, Parts A/B/C, 89–90: 46–55.

Su Y Z, Zhao W Z, Su P X, et al. 2007. Ecological effects of desertification control and desertified land reclamation in an oasis-desert ecotone in an arid region: A case study in Hexi Corridor, Northwest China. Ecological Engineering, 29(2): 117–124.

Tariq A, Graciano C, Sardans J, et al. 2022. Decade-long unsustainable vegetation management practices increase macronutrient losses from the plant-soil system in the Taklamakan Desert. Ecological Indicators, 145: 109653, doi: 10.1016/j.ecolind.2022.109653.

Tydecks L, Hernández-Agüero J A, Böhning-Gaese K, et al. 2023. Oases in the Sahara Desert-linking biological and cultural diversity. PLoS ONE, 18(8): e0290304, doi: 10.1371/journal.pone.0290304.

Wei X P, Pan X Y, Zhao C M, et al. 2008. Response of three dominant shrubs to soil water and groundwater along the oasis-desert ecotone in Northwest China. Russian Journal of Ecology, 39: 475–482.

Xie Y C, Gong J, Sun P, et al. 2014. Oasis dynamics change and its influence on landscape pattern on Jinta oasis in arid China from 1963a to 2010a: Integration of multi-source satellite images. International Journal of Applied Earth Observation and Geoinformation, 33: 181–191.

Xue J, Gui D W, Zhao Y, et al. 2016. A decision-making framework to model environmental flow requirements in oasis areas using Bayesian networks. Journal of Hydrology, 540: 1209–1222.

Xue J, Gui D W, Lei J Q, et al. 2018. Oasis microclimate effects under different weather events in arid or hyper arid regions: A case analysis in southern Taklimakan desert and implication for maintaining oasis sustainability. Theoretical and Applied Climatology, 137: 89–101.

Xue J, Gui D W, Lei J Q, et al. 2019. Oasification: An unable evasive process in fighting against desertification for the sustainable development of arid and semiarid regions of China. CATENA, 179: 197–209.

Yan J F, Chen X, Luo G P, et al. 2006. Temporal and spatial variability response of groundwater level to land use/land cover change in oases of arid areas. Chinese Science Bulletin, 51: 51–59.

Yang R J, Xu S C, Gu B J, et al. 2024. Stabilizing unstable cropland towards win-win sustainable development goals. Environmental Impact Assessment Review, 105: 107395, doi: 10.1016/j.eiar.2023.107395.

Yin X Y, Liu W, Zhu M, et al. 2023. Compounding effects of human activities and climatic changes on coexistence of oasis-desert ecosystems: Prioritizing resilient decision-making for a riskier world. Research in Cold and Arid Regions, 15(5): 219–229.

Zhang K C, An Z S, Cai D W, et al. 2017. Key role of desert-oasis transitional area in avoiding oasis land degradation from aeolian desertification in Dunhuang, Northwest China. Land Degradation & Development, 28(1): 142–150.

Zhang X F, Zhang Y F, Qi J H, et al. 2020. Evaluation of the stability and suitable scale of an oasis irrigation district in

Northwest China. Water, 12(10): 2837, doi: 10.3390/w12102837.

Zhang Y, Zhang K C, An Z S, et al. 2019. Quantification of driving factors on NDVI in oasis-desert ecotone using geographical detector method. Journal of Mountain Science, 16: 2615–2624.

Zhao C Y, Wang Y C. 2005. Study on spatial and temporal dynamic of soil water content in desert-oasis ecotone. Journal of Soil and Water Conservation, 19(1): 124–127. (in Chinese)

Zhao P, Qu J J, Xu X Y, et al. 2019. Desert vegetation distribution and species-environment relationships in an oasis-desert ecotone of northwestern China. Journal of Arid Land, 11: 461–476.

Zhao W Z, Chang X L. 2014. The effect of hydrologic process changes on NDVI in the desert-oasis ecotone of the Hexi Corridor. Science China Earth Sciences, 57: 3017–3117.

Zhou D Y, Wang X J, Shi M J. 2016. Human driving forces of oasis expansion in northwestern China during the last decade—A case study of the Heihe River Basin. Land Degradation & Development, 28(2): 412–420.

Zhou H, Zhao W Z, Zhang G F. 2017. Varying water utilization of *Haloxylon ammodendron* plantations in a desert-oasis ecotone. Hydrological Processes, 31(4): 825–835.